Material parameters for the structural dynamic simulation of electrical machines

M. van der Giet, K. Kasper, R.W. De Doncker, K. Hameyer

***Abstract*—Acoustic noise and vibration of electrical machines becomes increasingly relevant. The determination of equivalent mechanical material parameters of electrical steel is therefore necessary to bound the computational costs of the structural dynamic simulation to practical levels. An analytical model based on fundamental laws of mixture is compared to three different experimental approaches to from test objects. The following approaches are reviewed and compared: Static pressure test, ultrasonic measurements and the fitting of eigenfrequencies between measurement and Finite Element analysis. The forced vibration spectra show good agreement for the FEM fit and the ultrasonic approach. It verified that the FEM fit gives physically correct values.**

***Index Terms*—Acoustic noise, mechanical material parameters, Poisson ratio, ultra sound, vibration, Young's modulus**

I. Introduction

ACOUSTIC noise and mechanical vibration of electrical machines attract more and more interest in most application fields. A key to solving vibration problems in an early design stage is the accurate pre-calculation which can e.g. be done by a structural dynamic simulation.

Electrical machine stators, however, consist of heterogeneous mechanical materials: The stator sheet stack is made of laminated electrical steel, the winding of copper and resin for insulation purposes and mechanical strength of the end-winding region. For the structural modeling of electrical machines, it is essential to find equivalent mechanical material parameters which describe the structural dynamic characteristic of the homogenized material as close to the true behavior as possible for two reasons: Modeling and discretizing the mechanical structure with every possible detail, e.g. including every steel sheet and winding turn, would lead to impractically large numerical models.

The accuracy of the magneto-mechanically coupled numerical simulation relies on good estimates for the mechanical properties of the composite materials involved. The simplest approach is to use the values of the isotropic material properties of the corresponding material, i.e. steel for the laminated sheet stack. Another approach is to adjust the material properties such that the results of the numerical simulations fit the measurements. Both approaches have significant drawbacks: The first approach results in a poor accuracy of the numerical results. Although the second approach may work well for a specific application, the results may not be easily transferable to other machines since the optimization involved may hide all inaccuracies of the numerical model in the material parameters.

Four alternatives to using isotropic properties are found in the literature: Analytical modeling by means of basic mixture laws [1], static stress/strain-test [2], ultra sonic measurements [3] and fitting the numerical model [2]. All four approaches are applied and compared in terms of accuracy with respect to the forced vibration spectrum and in terms of physical meaning, especially in the case of parameter fitting. Since small and medium sized machines are often manufactured using bonding varnish technology for the electrical steel, the procedures need to be applicable to this kind of material as well. In order to reduce the influence of structure on the material properties, differently laminated cuboids are used as test specimen.

At the time the research was carried out all authors were with the University of Aachen. The static pressure test were supported by and performed at Aachen University of Applied Science.

M. van der Giet is currently with the Dr.-Johannes-Heidenhain GmbH, Traunreut, Germany. (email: vandergiet@heidenhain.de)

K. Kasper is with the Institute of Power Electronics and Electrical Drives (ISEA) of RWTH Aachen University, Germany (email: kr@isea.rwth-aachen.de)

R.W. De Doncker is with the Institute of Power Electronics and Electrical Drives (ISEA) of RWTH Aachen University, Germany (email: dd@isea.rwth-aachen.de)

K. Hameyer is with the Institute of Electrical Machine (IEM) of RWTH Aachen University, Germany (email: kay.hameyer@iem.rwth-aachen.de)

II. Devices under test

Three cuboids with nearly identical dimensions (70 mm times 30 mm times 380 mm) but with varying lamination were produced as test specimen, see Figure 1.

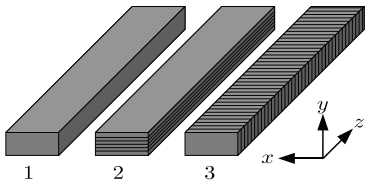

Figure 1: Schematic drawing of cuboids for equivalent material property determination.

Cuboid 1 is made of solid steel S235JRG2+C (formerly ST37K, specified in EN 10277/10278) and is used as a reference. The other two consist of 0.35 mm thick M250-35A sheet metal with bonding varnish on both sides. The lamination were cut with a plate shear and assembled to a stack in a clamping device. Print bars were used for adjustments. The clamped stacks were baked under pressure at 210 °C for four hours. After 24 hours of cooling a surface grinding machine was used to create a smooth surface. While cuboid 2 is laminated normally to the y-direction (coordinate system according to Figure 1), cuboid 3 is laminated normally to the z-direction.

III. Analytical modeling

Equivalent mechanical material properties of laminated sheets can be modeled analytically. Therefore, the fundamental

978-1-4673-0142-8/12/$26.00 ©2012 IEEE

rules of mixture which are presented in [1] for fiber reinforced material can be exploited. The composite material is considered to consist of two materials, one matrix material (index m) — in case of electrical steel this is the resin — and a fiber material (index f) which is the steel in this case. The volume ratio ϕ of fiber to matrix is the so called iron fill factor. This approach represents an approximation with the following assumptions: Small elastic strains, isotropy of the fiber material and of the matrix material, loads are only applied within the layer of consideration, ideal adhesion between fiber and matrix, uniform distribution of fibers in the matrix material and parallelism of the fibers to each other.

The quantities for which effective material parameters can be easily deduced are: mass density

$$\rho = \rho_\mathrm{f}\phi + \rho_\mathrm{m}(1-\phi)\,, \tag{1}$$

YOUNG'S modulus in direction of the fiber

$$E_\mathrm{p} = E_\mathrm{f}\phi + E_\mathrm{m}(1-\phi)\,, \tag{2}$$

YOUNG'S modulus perpendicular to the fiber

$$E_\mathrm{z} = \left(\frac{\phi}{E_\mathrm{f}} + \frac{1-\phi}{E_\mathrm{m}}\right)^{-1}, \tag{3}$$

POISSON ratio at a stress in the direction of the fiber

$$\nu_\mathrm{p} = \nu_\mathrm{f}\phi + \nu_\mathrm{m}(1-\phi)\,, \tag{4}$$

POISSON ratio at a stress perpendicular to the fiber

$$\nu_\mathrm{zp} = \nu_\mathrm{p}\frac{E_\mathrm{z}}{E_\mathrm{p}}\,, \tag{5}$$

and the effective shear modulus

$$G_\mathrm{zp} = \frac{G_\mathrm{m}G_\mathrm{f}}{G_\mathrm{m}\phi + G_\mathrm{f}(1-\phi)}\,. \tag{6}$$

For the M250 - 35A which is experimentally analyzed, the bulk material data is known from the manufacturer CD WÄLZHOLZ: E_f=207.5 GPa and ν_f=0.21. The values for the resin material could not be retrieved. Therefore, they are estimated as an average of plastic material: E_m=4 GPa and ν_m=0.35. The iron fill factor is estimated to be 95 %. Using equations (2) to (6), the resulting equivalent material parameters are obtained: E_p=197.3 GPa, E_z=58.6 GPa ν_p=0.22 ν_zp=0.64 and G_zp=22.3 GPa.

IV. EXPERIMENTAL DETERMINATION

A. Static tests

One way to measure elastic material properties is to apply a force and measure the resulting deformation in a static test. In [2], RAMESOHL already did static tests of claw-pole alternator stators where he found non-linear and hysteretic material behavior. The YOUNG'S modulus which was calculated was much smaller than that of solid steel.

For the paper presented here, a hydraulic press is used to apply a force to the cuboids and the change in length is measured for different loads, see Figure 2a, and a stress-strain diagram is derived. By means of a regression line, the average YOUNG'S modulus in z-direction can be determined.

To avoid bending of cuboid 2 in the press, the investigations are performed for cuboid 1 and 3 only. Figure 2b shows the

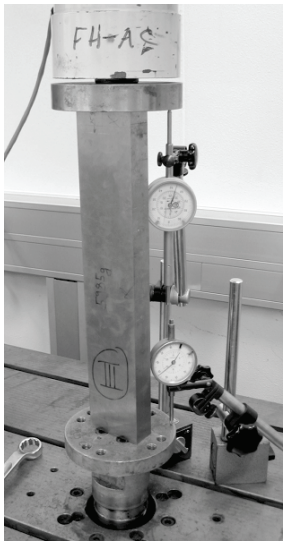

(a) Test setup for static measurement.

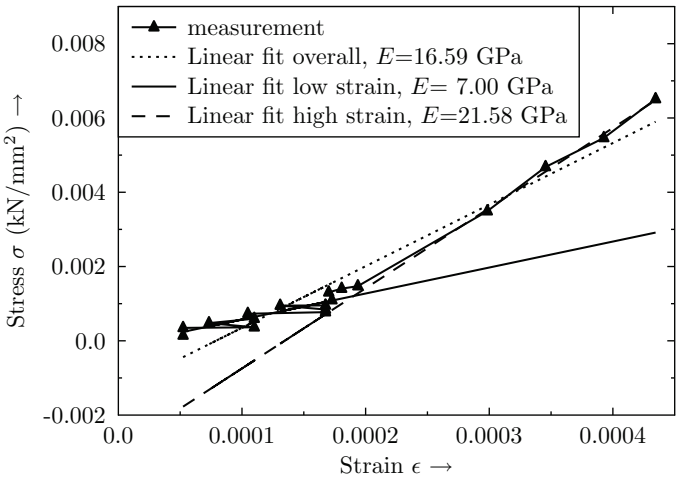

(b) Stress-strain diagram for cuboid 3 in z-direction.

Figure 2: Static tests.

derived stress-strain diagram for cuboid 3. For lower stress values, the strain shows strong fluctuations — most likely caused by inaccuracies of the applied pressure of the hydraulic cylinder. The line of best fit for the low-stress region leads to a rather low YOUNG'S modulus of 7 GPa. For higher stresses the measured values are more consistent and are all close to the line of best fit which yields a YOUNG'S modulus of 21.58 GPa. Cuboid 3 gets stiffer in z-direction with increasing load which is the same behavior obtained by RAMESOHL [2].

Since the pressures occurring due to vibration phenomena are much smaller (<0.001 GPa) than the test pressures (up to 0.01 GPa) applied here, the low strain best-fit would be applicable for the structural dynamic simulation of electrical machines. RAMESOHL find YOUNG'S modulus values much lower than solid steel without giving exact values. This relation between laminated steel sheet and solid steel is also found in this work. RAMESOHL further states that his static measurements lead to values close to dynamic measurement procedure. This however cannot be confirmed by the measurements in this

work as a comparison with ultrasonic and modal analyzes will show.

B. Ultrasonic measurements

TANG et al. [4], [3] only use isotropic modeling but present a measurement procedure for the (in-plane) YOUNG'S modulus of a laminated switched reluctance machine stator using ultrasonic transducers. This method is also used in [5] and is now applied to measure the YOUNG'S moduli of the cuboids in this paper, parallel and perpendicular to the lamination. Furthermore, the method is extended to take into account transverse isotropy.

Ultrasonic measurements are widely used in mechanical and material engineering for the detection of invisible faults (e.g. internal cracks) and also for elastic material property identification. The basic idea is to attach an ultrasonic transmitter to the test specimen and to create a short pulse of longitudinal waves (usually containing frequencies between 1 and 20 MHz) that travels through the material and is then detected by an ultrasonic receiver. From the measured time span between excitation and detection and the distance, the speed of sound c in the material can be calculated which depends on the material properties.

For a long homogeneous rod with a length much larger than the wavelength and a width much shorter than the wavelength, the speed of sound of longitudinal waves can be expressed as

$$c_{\mathrm{L}} = \sqrt{\frac{E}{\rho}\frac{1-\nu}{(1+\nu)(1-2\nu)}} \approx \sqrt{\frac{E}{\rho}} \tag{7}$$

with the YOUNG'S modulus E and the mass density ρ. If the width is larger than the wavelength, the POISSON ratio ν becomes significant and transverse waves occur, the speed of sound thereof can be calculated according to [6]

$$c_{\mathrm{T}} = \sqrt{\frac{G}{\rho}}. \tag{8}$$

For the transverse isotropic case , the speed of quasi-longitudinal waves can be derived for the xy-plane and the z-direction separately [7] as

$$\begin{aligned} c_{\mathrm{L}xy} &= \sqrt{\frac{1}{\rho^{\mathrm{m}}}\frac{E_x(E_x\nu_{xz}^2 - E_z)}{(1+\nu_{xy})(E_z\nu_{xy} - E_z + 2\nu_{xz}^2 E_x)}}, \\ c_{\mathrm{L}z} &= \sqrt{\frac{1}{\rho^{\mathrm{m}}}\frac{(\nu_{xy}-1)E_z^2}{E_z(\nu_{xy}-1) + 2\nu_{xz}^2 E_x}}. \end{aligned} \tag{9}$$

It should be noted that in anisotropic media in general, phase and group velocity are not identical. While all equations in this paper deal with the first, the latter velocities are measured with the ultrasonic method. However, along symmetry axes, both velocities are identical [7], so that this approach is valid.

Although the laminated test specimen are not homogeneous and the thickness of a single lamination layer is within the magnitude of the ultrasonic wavelength, TANG [4], [3] claims that equation (7) can be used as an approximation. Then the YOUNG'S modulus could be determined from the ultrasonic measurements as

$$E = \frac{(1+\nu)(1-2\nu)}{1-\nu}\rho c^2. \tag{10}$$

For the measurements a KRAUTKRÄMER USM 3S was used for pulse generation and detection. The transmitter was a KARL DEUTSCH S12H4, and the receiver an STS10WB10. The output bandpass filters of the pulse generator were set to 3 to 15 MHz. All cuboids were measured in $x-$, $y-$ and z-direction, leading to 12 measurement configurations. All configurations were measured several times at different locations on the test specimen and the results were averaged, they are listed in Table I Figure 3 exemplarily shows an inverted screenshot of the pulse generator during the measurement of cuboid 1 in y-direction. The excitation impulse is on the very left side, the second much smaller peak is the received pulse on the other side of the cuboid. The third peak is the twice reflected impulse that went through the test specimen three times.

Table I: YOUNG'S moduli determined by ultrasonic measurements

No.	Direction	c (m/s)	E (GPa)
1	x	5772	192
1	y	5587	180
1	z	5843	196
2	x	5646	176
2	y	4345	**104**
2	z	5328	157
3	x	5348	159
3	y	5529	169
3	z	-	-

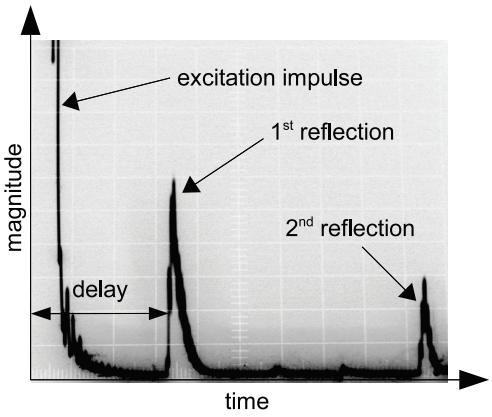

Figure 3: Screenshot of pulse generator.

The YOUNG'S moduli measured for the solid steel cuboid 1 are slightly lower than the data sheet value for steel which is 207 GPa. The value in the y-direction is lower than for the other directions which shows that the measurement accuracy is lower for short distances. The absolute reading error remains the same but the relative error increases. For the laminated cuboids, the YOUNG'S moduli in the lamination plane determined by the same approach as proposed in [4], [3] are significantly lower than those for solid steel and take values between 157 GPa and 176 GPa. In the rolling direction, the YOUNG'S modulus is around 160 GPa while it is approx. 170 GPa in perpendicular direction. So the rolling causes

a slight structural anisotropy. Since the orientation of the layers in electrical machines is usually varied to average out the effect of the magnetic anisotropy due to the rolling, the structural anisotropy can be ignored as well and an average value of approximately 165 GPa can be assumed for the in-plane YOUNG'S modulus E_p. This is a bit higher than the 152 GPa found by TANG [4], [3].

The most interesting result is the YOUNG'S modulus normal to the lamination layers, that could be measured for cuboid 2 only (here in y-direction), because for cuboid 3 the damping was so high that the entire energy of the pulse was absorbed and no signal could be received. TANG [4], [3] did not measure it at all, most likely because the actual machine stator design did not offer sufficient space on the front sheet to place the sensor, or because the active machine length of approx. 50 mm was already too long to permit ultrasonic measurements across all sheets. The value determined in this work was 104 GPa (printed in bold in the table in Figure 3), which is significantly lower than E_p but far higher than the YOUNG'S moduli in the axial direction found in [8], [9], [10], [11] for non-bonded stators.

The sensitivity of the results to variations of the POISSON ratio was investigated by varying it within a reasonable range. A 10 % increase of the POISSON ration leads to a 9 % decrease of the YOUNG'S modulus while a 10 % decrease causes a 7 % higher YOUNG'S modulus. Since this effect is rather small, the results of the measurements are not affected in principle. Thus, the results of the ultrasonic measurements according to [4], [3] can be summarized as follows: The in-plane YOUNG'S modulus of the bonded lamination E_p was determined as circa 165 GPa which is significantly lower than the value for solid steel, in most publications assumed as 207 GPa. Normal to the lamination the stiffness is lower, 104 GPa were measured for E_z.

However, especially the rather low YOUNG'S modulus parallel to the lamination is not expected. There is no reason why the steel's stiffness should decrease due to the lamination process considering the typically very high volume ratio ϕ of steel in the compound. To analyze this further, the wave propagation in transverse isotropic materials is investigated. Equation (9) gives the speed of sound in transverse isotropic media. It can be applied to the ultrasonic measurements. Unfortunately, there are too many unknown variables; hence, the equivalent material properties cannot be determined from the ultrasonic measurements using these equations. For this purpose, additional measurements of shear waves would be required for which no ultrasonic transducers were available. However, equation (9) can be applied once an entire set of material parameters is available to check whether the speed of sound is correctly modeled.

Furthermore, it becomes apparent that the YOUNG'S moduli calculated according to equation (7) have to be treated with caution for transverse isotropic media, especially when the values for E_z and E_p and ν_p and ν_zp differ significantly. Probably, the conclusion from the low speed of sound in the radial direction to a low YOUNG'S modulus in the radial direction by TANG [4], [3] is wrong. A similar reduction of the speed of sound compared to isotropic material can also be predicted by equation (9) assuming that E_p has a standard steel value, which seems to be more plausible, since the material parameters of the metal should not change due to the lamination procedure.

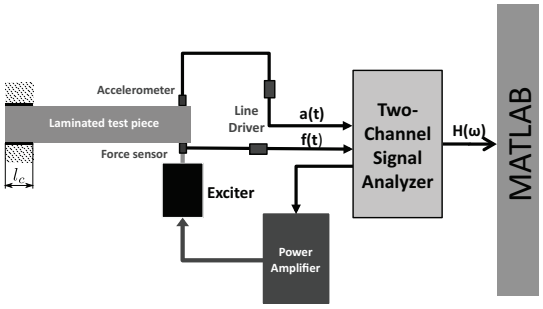

Figure 4: Schematics of the modal analyzes procedure.

C. Modal analysis and parameter fitting

a) Measurement of frequency-response-functions: A standard approach to the determination of equivalent mechanical material properties is the modal analysis of the system with a subsequent parameter fitting [12]. Force and acceleration measurement are performed to determine the resonance frequencies and eigenshapes of the single-side clamped cuboids. The values of the resonance frequencies are used as input parameters to an optimization procedure, in which a numerical modal analysis of the cuboid is computed. The equivalent mechanical material properties then are the result of this inverse problem.

The measurement set-up consists of a bench vice to clamp the cuboids. The clamping torque is adjusted using a torque wrench and kept constant at 80 Nm for all measurements. Two ways of clamping are used to measure vibration in $x-$ and in y-direction. The cuboid is excited with a vibration exciter (BK 4809) at the far end from the clamping and the acceleration is measured on the opposite side of the cuboid using an accelerometer (BK 4375). The force excitation is measured using a force gage (BK 8200). Both signals are first conditioned using two line drivers (BK 2644) and then fed to a two-channel spectrum analyzer (BK 2032) which is interfaced to and controlled by a MATLAB via the built-in IEEE 488 interface. The excitation signal is generated by the spectrum analyzer and fed through a power amplifier (BK 2718) to the exciter. Figure 4 shows the schematics of the modal analysis procedure.

White noise is used up to 12.8 kHz as force excitation signal. Figure 4 shows the schematics of the measurement procedure. The excitation position is kept constant at the cuboid center line at 25 mm from the end. In addition to measuring with the accelerometer placed straight on the opposite site of the exciter, a diagonal configuration is used to determine torsional vibration shapes. The measurement point of the accelerometer is moved along the cuboid by increments of 25 mm. The length of the clamping is l_c =63 mm.

The frequency-response-function (FRF) is measured for one excitation point $k = 0$ and different response locations l. The point-FRF, i.e. excitation and response are measured at the same location $k = l = 0$, is approximated here by placing both sensors on opposite sides of the cuboid, assuming that

Table II: SUMMARY OF EXTRACTED MODAL PARAMETERS.

No. i	Mode	cuboid 1		cuboid 2		cuboid 3	
		f_i (Hz)	η_i (%)	f_i (Hz)	η_i (%)	f_i (Hz)	η_i (%)
1	0. y	183	2.3	168	2.5	135	1.9
2	0. x	331	9.7	330	8.4	237	3.9
3	1. y	1187	4.0	1054	5.4	895	4.8
4	0. torsion	1529	1.0	1262	2.2	964	1.2
5	1. x	2264	3.7	2202	3.8	1726	2.5
6	2. y	3066	2.6	2715	2.6	2245	3.0
7	3. y	6371	7.9	6390	2.0	5746	4.1

the cuboid is rigid in this plane. Figure 5 shows the point-FRF for all three cuboids for the $x-$mode and for the y-mode measurements.

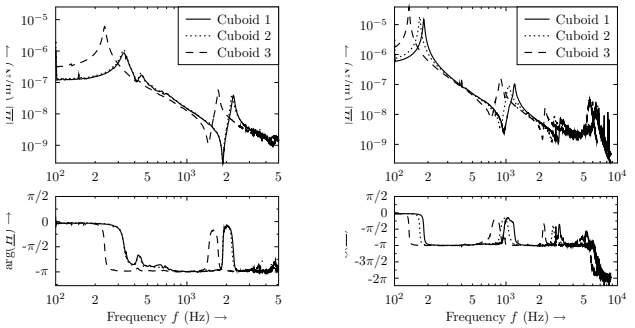

(a) x-mode. (b) y-mode.

Figure 5: Measured frequency response function of the three cuboids.

Following a standard single degree-of-freedom (SDOF) procedure using a circular fit of the FRF, the modal parameters of the cuboids are calculated to regenerate the FRF by the analytical model given by

$$\underline{\tilde{H}}_{kl}(\omega) = \frac{1}{-\omega M} + \sum_{i=1}^{N} \frac{\underline{A}_{kli}}{\omega_i^2 - \omega^2 + \mathrm{j}\eta_i\omega_i^2} + \frac{1}{K} \tag{11}$$

where K and M are constants to represent the modes that are outside the measured frequency band, ω_i is the resonance frequency of the i-th eigenmode, $\underline{A}_{kli}$ is the modal amplitude of mode i from location k to location l, and η_i is the damping coefficient of mode i.

Table II summarizes the results from the modal analyses. As the result from the modal analyses it can be stated that there are significant differences between solid steel and laminated steel. All measured damping ratios are below 10 %; hence the assumption to treat electrical steel as low damped material is confirmed. From Figure 6a it can be concluded that the input impedance of the bench vice is not varying strongly with frequency. Thus, a constant stiffness may be applied to the Finite Element (FE) model to clamp the cuboid.

From Figure 5a, it can be seen that the $x-$eigenmodes of cuboid 2 are very close to that of solid steel. Thus, it is confirmed that the in-plane properties of the compound material are dominated by the steel contribution. The difference of the FRF and of the mode shape's amplitude of cuboid 3 compared to cuboid one and two reveals significantly different material properties of the compound perpendicular to the lamination. The next step is to use the obtained data as input to a numerical optimization of the material parameters.

b) Finite-Element simulation: To find equivalent mechanical material parameters, a FEM based numerical modal analysis is performed. The software package ANSYS is used to solve the generalized eigenvalue problem. Figure 6b shows the FEM model together with the mass normalized eigenvector corresponding to the torsional vibration at the resonance frequency of $f = 916\,\mathrm{Hz}$. The model contains a total of 6472 first order octahedral elements with a total of 8198 nodes.

Comparing the experimentally determined resonance frequencies with the numerically simulated ones showed that the clamping using the bench vice cannot be modeled using a DIRICHLET boundary condition of zero displacement along the clamping length l_c. Therefore, the input impedance $\underline{\tilde{H}}_{11}(\omega)$ of the bench vice and the ground system is measured as a unidirectional FRF. The inverse of the FRF can be interpreted as a stiffness k which is shown in Figure 6a. Though the stiffness is not completely constant with respect to frequency, a mean value of $k = 10^8\,\mathrm{N/m}$ is used for the relevant frequency band. Using a constant k, spring elements of that value can be included in the FE analysis and a time consuming harmonic analysis is not necessary.

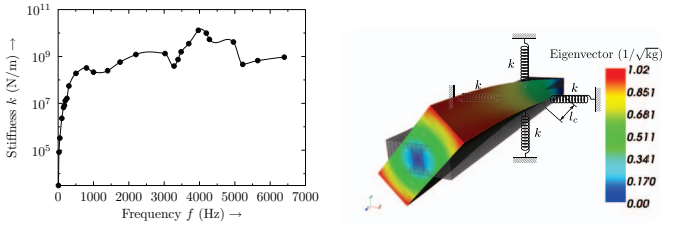

(a) Measured stiffness of bench vice. (b) Mass-normalized eigenvector at 916 Hz.

Figure 6: Finite-Element modeling.

c) Parameter-fitting: To achieve equivalent material properties that lead to the same vibrational behavior as the physical materials, an optimization problem is defined. The equivalent material properties $(E_\mathrm{p}, E_\mathrm{z}, \nu_\mathrm{p}, \nu_\mathrm{pz}, G_\mathrm{zp})$ are input quantities to the FEM problem and the resonance frequencies and mode shapes are result of the numerical modal analysis. The relative error $\epsilon_{\mathrm{r}i}$ between the numerically determined resonance frequency ω_i and the measured resonance frequency $\omega_{\mathrm{ref},i}$ of the i-th eigenmode is given by

$$\epsilon_{\mathrm{r}i} = \frac{\omega_i - \omega_{\mathrm{ref},i}}{\omega_{\mathrm{ref},i}}\,. \tag{12}$$

The objective function which is to be minimized is defined by the maximum of the squared relative error and the sum of squared relative errors for all considered eigenmodes

$$\mathbf{f}(\mathbf{x}) = \mathbf{f}\left((E_\mathrm{p}, E_\mathrm{z}, \nu_\mathrm{p}, \nu_\mathrm{pz}, G_\mathrm{zp})^\mathrm{T}\right) = \left(\max_{i=1\ldots7} \epsilon_{\mathrm{r}i}^2,\ \sum_{i=1}^{7} \epsilon_{\mathrm{r}i}^2\right)^\mathrm{T}. \tag{13}$$

Then, the optimization problem is to find the optimum o

$$\mathbf{f}(o) = \min\{\mathbf{f}(\mathbf{x}) | \mathbf{x} \in \Omega\}\,. \tag{14}$$

To ensure that the resonance frequency computed by the FEM corresponds to the same mode shape as the measured resonance when evaluating (12), the FEM eigenvector is sampled along the z-axis and the number of zero-crossings of the deformation shape is determined and compared to the measurement. The optimization can be performed for one cuboid at a time or for multiple cuboids at once. If the latter approach is chosen, a combined objective function is used.

In principle, any global optimization algorithm can be applied to find a parameter fit. In this paper, the differential evolution (DE) approach is chosen because it is fairly fast and reasonably robust. DE is a stochastic parallel direct search evolution strategy optimization method.

A total of twelve different optimization runs were performed which are summarized in Table III including the results (E_p,ν_p,E_z,ν_pz, and G_zp). The optimizations differ in the considered cuboid and the assumptions made and boundary constraints defined. The parameters used by the DE algorithm are given as follows: DE strategy: DE/rand/1 with per-generation-dither, number of iterations (generations) $g_\mathrm{max} = 60$, DE steps size $F = 0.35$, crossover probability constant $C_r = 0.9$, population size $N_p = 50$, and number of parameters N_D.

Line numbers 1, 5 and 7 are performed using the solid steel cuboid and are considered a plausibility check of the optimization. Simulations 1 to 3 used the laminate theory and preset values for the iron material properties (E_f and ν_f). For simulation 1, it is $E_\mathrm{f} = 210\,\mathrm{GPa}$ and $\nu_\mathrm{f} = 0.23$. A comparatively low value of the fill factor $\phi = 5\,\%$ is used to allow the optimization to be tested in finding the correct values for the majority of the material portion. It can be seen that the isotropic properties of the steel are found ($E_\mathrm{f} = 210\,\mathrm{GPa}$ and $\nu_\mathrm{f} = 0.23$, with a maximum frequency error of less then $4\,\%$. For lines number 5 and 6, the material parameter entries E_p and ν_p are given directly. Line number 7 gives the results for cuboid 1, with all parameter to be subject to optimization. It can be seen that for the solid cuboid the in-plane properties (E_p, and ν_p) can be traced back with reasonable accuracy, while for the transverse properties (E_z, ν_pz, G_zp), no physical correct solution can be obtained. This means that the inverse problem cannot be solved completely for isotropic materials or for material with a low degree of anisotropy.

In Lines 2 to 4, it is tried to find an estimate for the resin and it shows that a YOUNG'S modulus of approx. $E_\mathrm{m} = 10\,\mathrm{GPa}$ and a POISSON ratio of approx. $\nu_\mathrm{m} = 0.6$ can be considered for the resin. Comparing this to data known for plastic material, this seems realistic. In line 6, the bulk material of the steel sheet is used as an estimate for the in-plane properties. The resulting transverse YOUNG'S modulus fits well in the results from the other optimizations.

Lines 8 to 12 show the optimization results where all five parameters are left as subject to optimization. Lines 10 and 11 are re-runs of 8 and 9 with slightly different initial parameters and closer boundary constraints: Line 8 and 9: $E \in (50 - 150\ \mathrm{GPa})$ and Line 10 to 12: $E \in (150 - 230\ \mathrm{GPa})$. Because of the very low value of lines 9's in-plane YOUNG'S modulus, this run needs to be disregarded. Differences between cuboid 2 and 3 can be attributed to the slightly different manufacturing due to the different aspect ratio of the individual sheets.

It clearly shows that the optimization yields quite different sets of parameters that achieve similarly low errors. Some are obviously not realistic. So it is not trivial to determine *the* material parameters by this approach. Especially the POISSON ratios vary significantly; hence, the uncertainty concerning these values is the highest. However, the last line in Table III can be regarded as a conclusion, taking into account the optimization results and engineering knowledge.

V. COMPARISON

After equivalent material parameters have been extracted by four different methods, i.e. analytical mixture rules, static tests, ultra sonic measurements and FEM eigenvalue-fitting, the methods are compared in terms of forced vibration which is the application of such parameters in the acoustic analysis of electrical machines. Therefore, the FRF is computed by means of the FEM with different values of YOUNG'S moduli in the plane of the sheet and perpendicular to that, POISSON ratio and shear moduli are held constant as their influence has shown to be minor. Damping is assumed to be an average value of 7.5% for all eigenmodes. Figure 7 show the FRF for cuboid 2 and 3 in x-mode, comparing the measurement with the FEM using different material parameters.

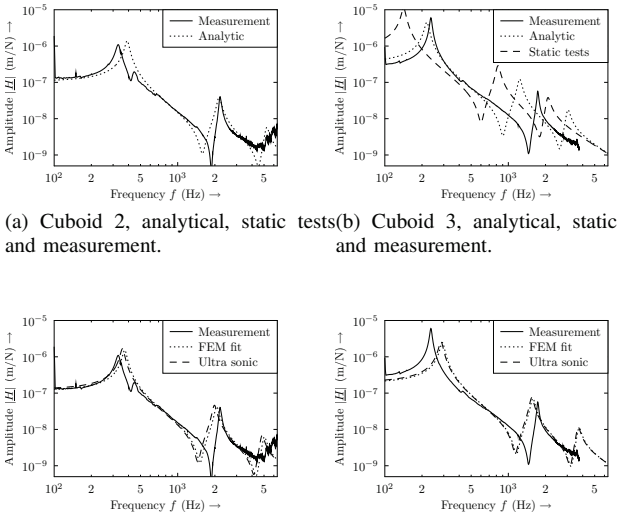

(a) Cuboid 2, analytical, static tests and measurement.

(b) Cuboid 3, analytical, static tests and measurement.

(c) Cuboid 2, FEM fit, ultra sonic and measurement.

(d) Cuboid 3, FEM fit, ultra sonic and measurement.

Figure 7: Comparison of FRF, FEM and measurement in x-mode.

As can be seen from Figures 7a and 7c, the agreement between measured FRF and simulated FRF is good in all cases. This is not surprising because the x-mode of that cuboid excites the sheets in the direction of the lamination, i.e. the vibrational behavior is not much different from that of a solid cuboid. As stated earlier a static compression test was only possible for cuboid 1 and 3. Comparing Figures 7b and 7d, it can be seen that the x-mode excitation which bends the cuboid across its lamination gives significantly different results for different material parameters. While the analytical determined material parameters set gives results that at least match the first resonance, the simulation data from the static test parameters is completely off. The simulation using parameters form

Table III: OPTIMIZATION RUNS AND RESULTS.

No.	Cub.	given	E_m	ν_m	E_p (GPa)	ν_p	E_z (GPa)	ν_pz	G_zp (GPa)	$\max \epsilon_i$ (%)
1	1	$E_\mathrm{f}, \nu_\mathrm{f}, \phi$	210.4	0.23	210.3	0.23	210.3	0.23	85.5	3.9
2	2	$E_\mathrm{f}, \nu_\mathrm{f}, \phi$	4.0	0.30	197.3	0.21	58.7	0.06	23.0	7.3
3	3	$E_\mathrm{f}, \nu_\mathrm{f}, \phi$	10.9	0.70	197.7	0.23	109.1	0.13	37.5	5.8
4	2,3	$E_\mathrm{f}, \nu_\mathrm{f}, \phi$	9.5	0.59	198.0	0.23	102.0	0.12	35.9	8.7
5	1	$E_\mathrm{p}, \nu_\mathrm{p}$	-	-	210.0	0.23	300.0	0.10	91.4	3.9
6	2,3	$E_\mathrm{p}, \nu_\mathrm{p}$	-	-	208.0	0.21	114.0	0.10	30.5	10.8
7	1	-	-	-	214.8	0.25	8.3	0.32	40.4	4.7
8	2	-	-	-	182.1	0.12	94.2	0.37	26.2	4.5
9	3	-	-	-	11.9	0.29	117.0	0.10	33.8	5.9
10	2	-	-	-	176.5	0.17	50.0	0.39	31.6	3.8
11	3	-	-	-	186.6	0.16	110.6	0.19	34.5	5.7
12	2,3	-	-	-	181.9	0.27	112.3	0.05	34.4	5.5
					180	0.2	110	0.15	32	

ultrasonic measurement and FEM fit are almost equal and show good agreement with the measured FRF also for this case. This gives rise to two conclusions: On the one hand, it is shown that ultrasonic and FEM fit can both be recommended for practical application, what ever is more convenient. It is expected that ultrasonic are more appropriate for sheet samples whereas FEM fit would be more commonly used for ready built stator structures. On the other hand, it shows that the procedure of fitting the eigenfrequencies of laminated steel structure between FEM simulation and measurement can give physically correct results as they are validated by means of the ultrasonic measurement here.

VI. SUMMARY AND CONCLUSIONS

This paper studies the determination of equivalent mechanical material parameters of electrical steel which is necessary to bound the computational costs of the numerical simulation to practical levels. An analytical model based on fundamental laws of mixture is presented. Subsequently, three different experimental approaches to determine equivalent mechanical material properties for laminated electrical steel sheets from test objects are reviewed and compared.

First, static tests are shown that allow for a direct determination of the stiffness from the measurement of force and deformation. Due to non-linear behavior of the bonding varnish, this approach is not successful. Second, ultrasonic probes are used to determine the speed of sound in different directions of the test specimen, and equations to link the transverse isotropic material properties to these speeds are derived. However, the problem remains under-determined (2 measured speeds, 5 parameters). Finally, experimental modal analyzes are used to determine the eigenmodes and eigenfrequencies of the test objects. Then, the equivalent material properties for a structural finite element model are automatically optimized until the computed eigenfrequencies fit the measured ones. A comparison of forced vibration spectra shows good agreement for the FEM fit and the ultrasonic approach. It verified that the FEM fit gives indeed physically correct values.

As a future study, it is interesting to include the damping properties of the material in the analysis. Therefore, a consideration of the amplitudes of vibration and/or the bandwidth of the eigenmodes can be employed in the optimization. Additionally, the application of both approaches, ultrasonic and FEM fit, to different steel grades and resin materials may be of interest as well as the influence of additional processing such as welding or stamping.

REFERENCES

[1] H. Altenbach, J. Altenbach, and R. Rikards, *Einführung in die Mechanik der Laminat- und Sandwichtragwerke*. Deutscher Verlag für Grundstoffindustrie Stuttgart - Modellierung und Berechnung von Balken und Platten aus Verbundwerkstoffen, 1996.

[2] I. Ramesohl, G. Henneberger, S. Kuppers, and W. Hadrys, "Three dimensional calculation of magnetic forces and displacements of a claw-pole generator," *IEEE Transactions on Magnetics*, vol. 32, no. 3, pp. 1685–1688, 1996.

[3] Z. Tang, P. Pillay, A. Omekanda, C. Li, and C. Cetinkaya, "Young's modulus for laminated machine structures with particular reference to switched reluctance motor vibrations," *IEEE Transactions on Industry Applications*, vol. 40, no. 3, pp. 748–754, 2004.

[4] Z. Tang, P. Pillay, A. M. Omekanda, C. Li, and C. Cetinkaya, "Effects of material properties on switched reluctance motor vibration determination," in *Industry Applications Conference, 2003. 38th IAS Annual Meeting. Conference Record of the*, vol. 1, October 2003, pp. 235–241.

[5] W. Cai, P. Pillay, Z. Tang, and A. M. Omekanda, "Low-vibration design of switched reluctance motors for automotive applications using modal analysis," *IEEE Transactions on Industry Applications*, vol. 39, no. 4, pp. 971–977, July 2003.

[6] B. P. L. Cremer, M. Heckl, *Structure-Borne Sound*. Springer-Verlag Berlin Heidelberg, 2005.

[7] G. Mavko, T. Mukerji, and J. Dvorkin, *The Rock Physics Handbook: Tools for Seismic Analysis of Porous Media*, 2nd ed. Cambridge University Press, 2009.

[8] S. Garvey, "The vibrational behaviour of laminated components in electrical machines," in *Fourth International Conference on Electrical Machines and Drives*, 1989, pp. 226–231.

[9] K. Williams and H. Wang, "The effect of laminations on the vibrational modes of circular annular plates," *Experimental Mechanics*, vol. 33, no. 2, pp. 180–186, June 1996.

[10] H. Wang and K. Williams, "Effects of laminations on the vibrational behaviour of electrical machine stators," *Journal of Sound and Vibration*, vol. 202, no. 5, pp. 703–715, 1997.

[11] H. Wang, "Experimental study of vibrational behavior of laminated annular disks," *The Journal of the Acoustical Society of America*, vol. 111, no. 4, pp. 1701–1708, 2002.

[12] M. Link, "Was kann man von rechnerisch auf testdaten angepassten finite-elemente modellen erwarten," in *VDI Berichte 1550 Experimentelle und rechnerische Modalanalyse sowie Identifikation dynamsicher Systeme*. VDI Verein Deutscher Ingenieure, June 2000, pp. 73 – 94.